Emission from Zeolite-Occluded Manganese–Diimine Complexes

Peter-Paul H. J. M. Knops-Gerrits, Frans C. De Schryver, Mark van der Auweraer, Hans Van Mingroot, Xiao-yuan Li and Pierre A. Jacobs*

Abstract: Manganese complexes of 2,2′-bipyridine (bpy) and 1,10-phenantroline (phen) have been synthesised in the supercages of cubic NaX and NaY and in the hypercages of the hexagonal NaEMT faujasites. The coordination and redox chemistry were studied with ESCA, CA, FT-IR, FT-Raman, diffuse reflectance and emission techniques. FT-IR/FT-Raman shows *cis* coordination for all complexes and a high Mn–N stretching frequency in the phen complexes as a result of steric constraints imposed by the ligand. $[Mn(bpy)_2]^{2+}$ in the different zeolites shows metal-to-ligand charge transfer (MLCT; at 495 nm); for $[Mn(phen)_2]^{2+}$-NaY the MLCT is broadened owing to complex distortion. On MLCT excitation $[Mn(bpy)_2]^{2+}$ complexes show an ipsochromic shift in the emission and an increase in quantum yield with increasing steric restrictions imposed by the zeolite. The ipsochromic shift of the emission band of $[Mn(phen)_2]^{2+}$ in NaY results from the combined effect of the ligand field (this suggests emission from a CT state) and of coordinative distortion. The key factor influencing the emission properties is found to be the overall matrix-induced complex distortion. Cation stabilisation of the ligand anion affects emission indirectly. The decay times for $[Mn(bpy)_2]^{2+}$-NaY are in the millisecond range (7.5–11.5 ms). A proposed model for excitation and emission properties of zeolite-occluded Mn^{II} complexes involves excitation of a quartet CT state, intersystem crossing and subsequent emission. The enhanced stability of the coordination sphere in the zeolite allows complexes to luminesce from a CT state, which is not detected in solution. The zeolite behaves as a supramolecular cryptating agent, protecting complexes from photodissociation.

Keywords
charge transfer complexes · diimine complexes · emission spectroscopy · manganese complexes · zeolites

Introduction

Although Mn complexes in solution or on supports have been studied in detail by spectroscopic techniques,[1] their photophysical properties are still not very well understood.[2–4] Polypyridine ruthenium complexes, such as $[Ru(bpy)_3]^{2+}$ or *cis*-$[Ru(bpy)_2]^{2+}$ (bpy = 2,2′-bipyridine), have been extensively studied in this respect.[5–6, 8–9] Complexes of Ru^{II}, Os^{II}, Cr^{III}, Rh^{III} and Ir^{III} are the only species known to luminesce strongly in solution at room temperature and to exhibit good photosensitisation capacity for electron- and energy-transfer processes. An overview of the photophysical, photochemical and electrochemical properties of such systems is available.[5] Occlusion of Ru^{II} tris and bis complexes in zeolites has been described by Mallouk et al.,[6f–h] Lunsford et al.,[7] Dutta et al.[8] and Kincaid et al.[9]

Emission properties of O- and N-ligand Mn^{II} complexes have been reported.[2–4] At room temperature octahedral Mn octamethylpyrophosphoramide complexes $[Mn(OMPA)_3(ClO_4)_2]$[2d] show a broad phosphorescence band centred at 585 nm, which is red-shifted at lower sample temperatures. At liquid-nitrogen temperature it is situated at 620 nm and is assigned to a $^4T_1 \rightarrow {}^6A_1$ transition. Tetrahedral Mn^{II} in the cubic sites of different inorganic lattices, such as ZnS, ZnSe and ZnTe, has been characterised by emission spectroscopy.[2c] Ligand variation shows that the governing effect on the decay time of the Mn^{II} $^4T_1 \rightarrow {}^6A_1$ emission is the spin–orbit interaction of the p electrons of the ligands with Mn^{II}. Excitation and emission luminescence spectra for complexes of Mn^{II} halide with 2,6-dimethylpiperidinium and *N*-methylpiperidine have been published as well.[2a–b] In permanganate (MnO_4^-) tetrahedral Mn^{VII} is bound by four oxygen ligands and does not luminesce.[3]

The photoprocesses of complexes of Mn^0 with carbonyl and α-diimine ligands have recently been reported by Stufkens et al.[4] Mononuclear 16-electron ligand-centred radicals of $[Mn(\alpha\text{-diimine})(CO)_3]$ with a π^* singly occupied molecular orbital (SOMO) are formed upon excitation. In these low-spin Mn^0 complexes the six electrons are in the t_{2g} levels, and an electron is excited either into the d_{z^2} orbital for pentacarbonyl or into the π^* orbital for tricarbonyl/α-diimine complexes.

Occlusion of $[Mn(bpy)_2]^{2+}$ complexes in zeolite Y has recently been reported and leads to mainly *cis*-$[Mn(bpy)_2]^{2+}$ complexes.[1] The present work describes our attempt to understand

[*] Prof. Dr. Ir. P. A. Jacobs, Ir. P. P. Knops-Gerrits
Centrum voor Oppervlaktechemie en Katalyse, Katholieke Universiteit Leuven
Kardinaal Mercierlaan 92, 3001 Heverlee (Belgium)
Fax: Int. code +(16)321998
e-mail: pierre.jacobs@agr.kuleuven.ac.be
Prof. Dr. F. C. De Schryver, Prof. Dr. M. van der Auweraer, H. Van Mingroot
Chemistry Department, Katholieke Universiteit Leuven
Celestijnenlaan 200F, B-3001 Heverlee (Belgium)
Prof. Dr. X.-Y. Li
Chemistry Department, Hong Kong University of Science and Technology
Clear Water Bay (Hong Kong)

0947-6539/96/0205-0592 $ 15.00+.25/0

steric influences around the Mn^{2+} ion by ligating it to 2,2′-bipyridine and 1,10-phenantroline in zeolite cages of different sizes and with a different numbers of charge-compensating cations. The change of zeolite topology is the first factor used for steric variation. $[Mn(bpy)_2]^{2+}$ was therefore synthesised in the hypercages of a hexagonal faujasite and the supercages of cubic faujasite. To obtain coordination geometries with different degrees of distortion imposed by the ligand, occlusion of $[Mn(bpy)_2]^{2+}$ and $[Mn(phen)_2]^{2+}$ within NaY was compared. Fine-tuning of steric effects was achieved by changing the number of charge-compensating cations, that is, by comparing the occluded complexes in zeolite NaX and NaY. The emission spectra of the Mn complexes are reported, and the effects of coordination and sterochemistry on these spectra are discussed.

Experimental Procedure

Synthesis of materials: Hexagonal faujasite with EMT topology (NaEMT) which was free of significant cubic intergrowths was synthesised according to a literature procedure [16a]. After being washed with deionised water and dried at 333 K, the crystals were calcinated in a muffle furnace at 823 K for 20 h. The hydrogel prepared with Ludox HS-40 (Du Pont), Gibsite (Fluka), NaOH pellets (Merck) and 18-crown-6 ether (Janssen Chimica) was aged at 293 K for 3 d. The Si/Al ratio of the material was 3.50. Cubic faujasites with different Si/Al ratios [NaX (1.04), NaY (2.45)] were obtained from Zeocat.

Synthesis of complexes: The synthesis of $[Mn(bpy)_2]^{2+}$ in NaX, NaY and NaEMT, and of $[Mn(phen)_2]^{2+}$ in faujasite NaY were performed as previously described for $[Mn(bpy)_2]^{2+}$ in NaY [1,11]. After cation exchange of Mn^{2+} for Na^+, at a loading of one Mn^{2+} per supercage for faujasite X and Y and one Mn^{2+} per hypercage for faujasite EMT, the samples were dehydrated at 473 K and subsequently mixed at 298 K with bpy or phen at a 2.5:1 ligand-to-metal ratio under N_2 atmosphere. Ligands were sorbed on the zeolite by solid-state mixing at 363 K for 48 h. The samples were soxhlet extracted in dichloromethane for 24 h to remove uncomplexed ligand.

Thermogravimetric analysis was performed with a Setaram-92 balance. Samples were heated under 5 vol% of O_2 in a helium atmosphere at a rate of 5 K per minute.

XPS (X-ray photoemission spectroscopy) measurements were performed with a Perkin-Elmer PHI 5500-5600 apparatus (using monochromatic $Al_{K\alpha}$ X radiation, 1486.6 eV) in the 0–1400 eV window at $1.33\ 10^{-10}$ Pa. The calibration values used are: Mn(2p 3/2): 639.6 eV (S. F. 150.146); Al (2p): 71.2 eV (S. F. 19.719); Si (2p): 99.7 eV (S. F. 28.827).

Chemical analysis (CA) measurements were performed with a Varian Liberty 100 ICP-emission spectroscopy apparatus.

FT-IR spectra were recorded on a Nicolet 730 spectrometer. KBr pellets containing the zeolite powders were used.

FT-Raman spectra were recorded on a Brucker IFS-1000 spectrometer using 1000 scans at 100 mW laser power.

Molecular modelling was performed with the program Hyperchem V 3.0 for Windows (Auto-desk), using a completed version of the MM + force field, that is, a completed version of Allinger's MM2 [13a]. The zeolite lattice coordinates used were derived from Rietveld refined X-ray diffraction studies of faujasites Y and EMT ([13b], and references therein). The coordinates of pseudooctahedrally coordinated *cis*-$[Mn(bpy)_2]^{2+}$ were obtained from an XRD study [13c]. The symmetry of tris(diimine) and *cis*-bis(diimine) complexes in the ground state are D_3 and C_2, respectively. Excited states(e.g., $^4T_1$) were simulated with O_h symmetry as six-coordinate pseudospherical complexes.

Diffuse reflectance spectra (DRS) were recorded in the 200–800 nm range with a Cary 5 instrument, a type I diffuse-reflectance attachment and an Eastman Kodak white reflectance standard. The spectra were computer-processed with intensity scales in arbitrary units.

Luminescence spectroscopy: The front-face stationary emission spectra of powder samples were recorded with an SPEX Fluorolog model 1691 apparatus with a double monochromator (SPEX spectramate 1980 B) in the 300–800 nm range with excitation at wavelengths corresponding to positions of the CT maxima. The samples were pretreated in vacuum and kept at 1.3 Pa during the measurements. The spectra are uncorrected for spectrometer response, and intensity scales are arbitrary. Quantum-yield (Φ) determination was based on calibration with $[Ru(bpy)_3]^{2+}$, for which Φ approaches unity [10a–c]. It should be stressed that the measurements for zeolite-occluded species occur on samples with much higher concentrations (around 0.88 M or eight complexes per unit cell) than in solution (usually 10^{-5} M).

Time-resolved emission measurements were obtained by excitation with a Spectra Physics Quanta-Ray DCR 3A pulsed Nd:Yag laser coupled to a temperature-controlled HG-2 harmonic generator with a PHS-1 prism harmonic separator from which the second (532 nm, 360 mJ, 6 ns) and the third (355 nm, 160 mJ, 5 ns) harmonics were used. A high-voltage pulse generator (Princeton Applied Research, model 1302 fast pulser 5–10–20 ns gate) and gated intensifier coupled with a silicon photodiode array detector (Princeton Applied Research, model 1421) were used to create a delay (ranging from 100 ns to 40 ms) between the excitation pulse and the detection time window (of 1 μs). The spectrum was analysed in the 200–700 nm domain by using an OMA-3 console with data-processing unit.

Results

Intrazeolitic complexation of Mn by diimines was performed by a stepwise method comparable to that previously reported for the synthesis of $[Mn(bpy)_2]^{2+}$ in NaY zeolites.[1] There is a major difference between the cage structure in cubic and hexagonal faujasites. Molecular graphics tells us that complex retention occurs in the supercages of cubic and the hypercages of hexagonal faujasite (see Fig. 6 below). Although two types of cages exist in the latter topology,[16c] for steric reasons only the larger hypercages with a free diameter of around 1.3×1.4 nm and with five 12-membered ring (12 MR) apertures are suitable for synthesis of the complexes. The smaller hypocages with three 12 MR apertures are too small for complex fixation.

Thermogravimetric analysis showed that, after extraction of MnNaY loaded with ligand, the average number of remaining ligands per Mn ion does not differ significantly from 2, which corresponds to the proposed stoichiometry for the complex (Table 1). With NaX a small amount of residual bpy ligand remains, while a small amount of uncomplexed Mn^{2+} seems to be present with NaEMT. The chemical analyses (Table 2) and XPS results (Table 3) show that silicon is enriched at the surface of these three zeolites. The Mn/Si ratios obtained with XPS and chemical analysis is similar for both Y and X zeolites. This is a clear indication that significant amounts of complex do not

Table 1. Thermogravimetric analysis of zeolite-occluded $[Mn(L)_2]^{2+}$ complexes before (a) and after (b) soxhlet extraction.

	L/Mn (a)	L/Mn (b)
$[Mn(bpy)_2]^{2+}$-NaX	2.46	1.74
$[Mn(bpy)_2]^{2+}$-NaY	2.52	2.02
$[Mn(bpy)_2]^{2+}$-NaEMT	2.43	2.27
$[Mn(phen)_2]^{2+}$-NaY	2.49	2.14

Table 2. Chemical analysis of zeolite-occluded $[Mn(L)_2]^{2+}$ complexes after extraction.

	Mn:Si	Mn:Al	Al:Si
$[Mn(bpy)_2]^{2+}$-NaX	0.141	0.058	0.962
$[Mn(bpy)_2]^{2+}$-NaY	0.060	0.138	0.407
$[Mn(bpy)_2]^{2+}$-NaEMT	0.042	0.196	0.286
$[Mn(phen)_2]^{2+}$-NaY	0.067	0.144	0.409

Table 3. XPS analysis of zeolite-occluded $[Mn(L)_2]^{2+}$ complexes after extraction.

	Mn:Si	Mn:Al	Al:Si
$[Mn(bpy)_2]^{2+}$-NaX	0.117	0.084	0.794
$[Mn(bpy)_2]^{2+}$-NaY	0.049	0.199	0.248
$[Mn(bpy)_2]^{2+}$-NaEMT	0.080	0.365	0.218
$[Mn(phen)_2]^{2+}$-NaY	0.060	0.300	0.199

  0947-6539/96/0205-0593 $ 15.00+.25/0

remain adsorbed at the external surface of the crystals.[18,b] This is not the case with EMT. Given the Al depletion in the crystal rim and the heterogeneity in site population across the crystal,[16,d] the data cannot be directly rationalised. Scanning electron microscopy (SEM) photographs of $[Mn(bpy)_2]^{2+}$ in NaY and NaX[1] confirmed the absence of crystals of the $[Mn(L)_2]^{2+}$ complexes at the outer surface. With NaEMT similar pictures are obtained (Fig. 1).

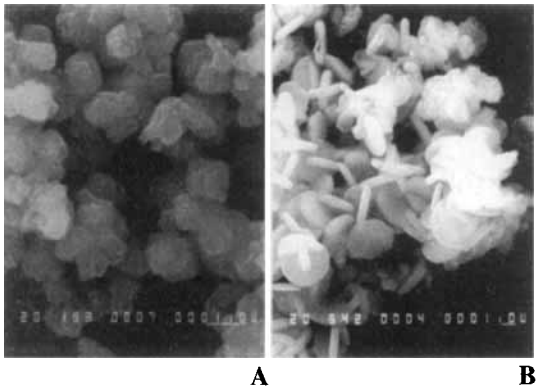

A B

Fig. 1. Scanning electron micrographs of the cubic and hexagonal faujasite NaY (A) and NaEMT (B) containing $[Mn(bpy)_2]^{2+}$ complexes.

***cis/trans* Biscomplexation of diimine-containing zeolites:** FT-IR spectra of $[Mn(bpy)_2]^{2+}$ in NaX, NaY and NaEMT (Table 4) show only minor frequency shifts for all vibrations relative to that of the homogeneous *cis*-$[Mn(bpy)_2]^{2+}$ complex.[1] The frequencies for $[Mn(bpy)_2]^{2+}$ in EMT closely resemble those of the homogeneous complexes. The $[Mn(bpy)_2]^{2+}$ complexes encaged in NaX and NaY zeolites contain mainly *cis* and little *trans* isomer. The spectra of homogeneous *cis*- and *trans*-bipyridyl complexes differ only in the out-of-plane C–H deformation bands at 757(m) and 772(s) cm^{-1}: the symmetrical $[Mn(bpy)_3]^{2+}$ (D_{3h}) and *trans*-$[Mn(bpy)_2]^{2+}$ (D_{2h}) show a single band for the C–H out-of-plane deformation; when the symmetry is lowered as in *cis*-$[Mn(bpy)_2]^{2+}$ (C_2), this strong vibration is split into two bands of medium intensity. For $[Mn(bpy)_2]^{2+}$-NaY complexes a broad maximum occurs at 772 cm^{-1} with a shoulder at 768 cm^{-1}, indicative of a major fraction of *cis*-coordinated complexes (Table 4). For $[Mn(phen)_2]^{2+}$-NaY complexes, the out-of-plane C–H deformations (Fig. 2B) also point to *cis* coordination. Two different out-of-plane C–H deformations of the aromatic ring hydrogens are observed—at 848 cm^{-1} for the central ring and at 725 cm^{-1} for the pyridyl ring.[6d] The spectra of homogeneous *cis*- and *trans*-$(phen)_2$ complexes again differ in the out-of-plane C–H deformation bands, as a result of their different symmetry. Although the splitting is better resolved for the 725 cm^{-1} band (to 723 and 729 cm^{-1}) than for the 848 cm^{-1} band, the spectrum again points to the presence of *cis*-coordinated complexes (Fig. 2A).

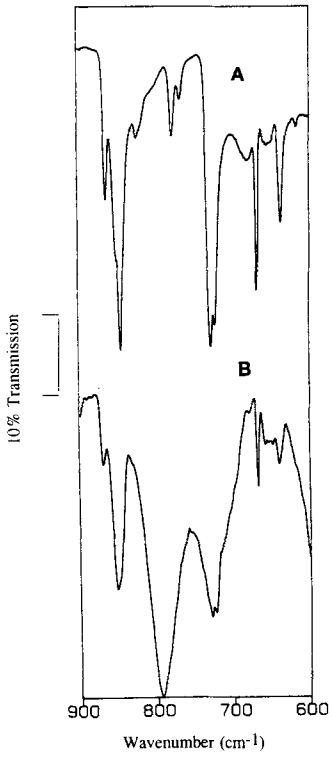

Fig. 2. FT-IR Spectra in the C–H out-of-plane deformation region for *cis*-$[Mn(phen)_2(NO_3)_2]$ (A) and $[Mn(phen)_2]^{2+}$-NaY (B).

In FT-Raman the M–N bands occur in the 180–290 cm^{-1} region for metals with partially filled e_g orbitals such as Mn^{II}.[6d] For $[Mn(bpy)_2]^{2+}$-NaY this band, which is a combination mode of the Mn-N-C deformation and the Mn–N stretch modes, is observed at 243 cm^{-1} (Fig. 3B). Owing to the steric constraint in $[Mn(phen)_2]^{2+}$-NaY, the Mn–N stretch frequency is shifted to 251 cm^{-1} (Fig. 3A).

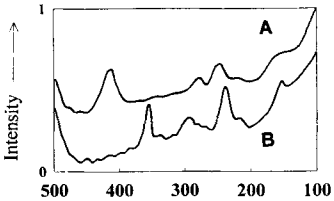

Fig. 3. FT-Raman spectra in the Mn–N stretch region of $[Mn(phen)_2]^{2+}$-NaY (A) and $[Mn(bpy)_2]^{2+}$-NaY (B).

Coordination of Mn^{2+} in $[Mn(bpy)_2]^{2+}$-NaX/NaY/NaEMT and $[Mn(phen)_2]^{2+}$-NaY: The reflectance spectrum of $[Mn(bpy)_2]^{2+}$-NaY (Fig. 4, left, spectrum a) shows MLCT maxima at 495 nm with a shoulder at 530 nm. Since it is a high-spin complex,

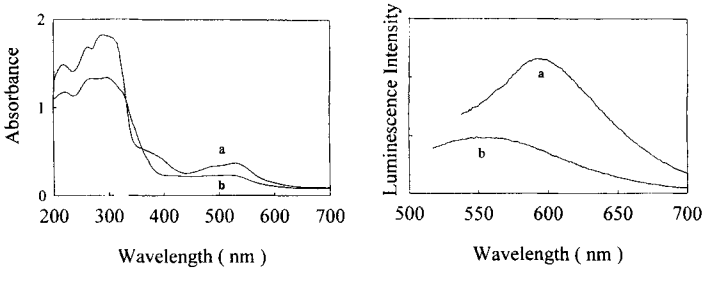

Fig. 4. DRS (left) and emission spectra (right) at 490 nm excitation of $[Mn(bpy)_2]^{2+}$-NaY (a) and $[Mn(phen)_2]^{2+}$-NaY (b).

Table 4. FT-IR wavenumbers of *cis*-$[Mn(bpy)_2(NO_3)_2]$ and *cis*-$[Mn(bpy)_2]^{2+}$-NaY [a].

Assignment	Homog.[b]	FAU-X	FAU-Y	EMT
in-plane ring deformation	623 (m)	628 (m)	634 (w)	627 (m)
in-plane ring deformation	667 (s)	667 (s)	668 (s)	667 (s)
out-of-plane ring and C–H deformations	735 (s)	736 (m)	737 (m)	736 (m)
out-of-plane C–H deformation #1	757 (m)	756 (sh)	757 (sh)	
out-of-plane C–H deformation		765 (s)	768 (sh)	765 (sh)
out-of-plane C–H deformation #2	772 (s)	771 (sh)	772 (s)	771 (s)
in-plane C–H deformation	1305 (m)	1317 (m)	1317 (m)	1315 (m)
ring stretch (C=C/C=N stretch)		1436 (s)	1435 (s)	
ring stretch (C=C/C=N stretch)	1440 (s)	1444 (vs)	1442 (vs)	
ring stretch (C=C/C=N stretch)	1473 (m)	1474 (s)	1475 (s)	1473 (sh)
out-of-plane ring and C–H deformations	1490 (m)	1492 (m)	1493 (m)	1491 (m)
ring stretch (C=C/C=N stretch)	1568 (m)	1567 (vw)	1568 (vw)	1567 (vw)
ring stretch (C=C/C=N stretch)	1574 (m)	1576 (w)	1577 (w)	1575 (ω)
ring stretch (C=C/C=N stretch)	1594 (s)	1596 (s)	1597 (s)	
ring stretch (C=C/C=N stretch)		1605 (s, sh)	1606 (s)	1602 (s)

[a] Zeolite pore-stretching, bending and pore-breathing vibrations of the FAU and EMT zeolites are omitted for clarity [13b]. [b] The homogeneous *cis*-$[Mn(bpy)_2(NO_3)_2]$ were synthesised according to ref. [13c]; *cis* or *trans* coordination only has a significant effect on the splitting of the bpy C–H out-of-plane vibration, not on the nitrate bands.

0947-6539/96/0205-0594 $ 15.00+.25/0 Chem. Eur. J. 1996, 2, No. 5

a significant degree of π backbonding occurs. It is hardly possible to identify the d–d bands of the Mn^{2+} complex, since they can even be obscured by the very weak UV organic absorption tailing into the visible. The excitation spectra are comparable to the diffuse reflectance spectra.

For $[Mn(phen)_2]^{2+}$-NaY a broadened MLCT region is observed (Fig. 4, left, spectrum b), owing to the structural rigidity of the ligand. No deformation of the ligand from its flat conformation is allowed; a distortion of the coordination sphere occurs as a result, and the coordinative environment is thus less well defined than in case of the more flexible bipyridine ligand.

The intensity decrease of the MLCT absorptions (Fig. 5, left) in the order NaX > NaY > NaEMT can be rationalised as follows: since the Si/Al ratio of the zeolite increases in the same direction, the walls of the large cages show a decreasing Na cation population.

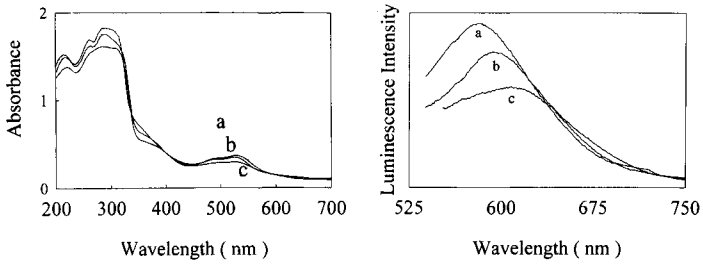

Fig. 5. Effect of zeolite topology and composition on the DRS (left) and emission spectra (right) at 490 nm excitation: $[Mn(bpy)_2]^{2+}$-NaX (a), $[Mn(bpy)_2]^{2+}$-NaY (b) and $[Mn(bpy)_2]^{2+}$-NaEMT (c).

Molecular models of the complexes in the FAU (X,Y) supercages and EMT hypercages are shown in Figure 6.

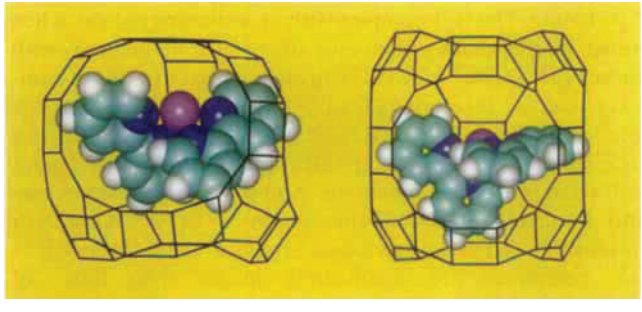

Fig. 6. Space-filling molecular models of the $[Mn(bpy)_2]^{2+}$ complexes in FAU (left) and EMT (right) topologies.

MLCT emission occurs by excitation of the MLCT state: The $[Mn(bpy)_2]^{2+}$-NaY complexes in the zeolites show straightforward MLCT characteristics. Mn^{II} complexes are fairly ionic, in part due to their zero crystal field stabilization energy. With excitation at 490 nm, the emission maximum for the $[Mn(bpy)_2]^{2+}$-NaY (Fig. 4, right, spectrum a) complexes is at 580 nm ($\Phi = 0.045$), while for $[Mn(phen)_2]^{2+}$-NaY (spectrum b) it is at 555 nm ($\Phi = 0.019$). The lowering of quantum yields observed in the latter case reflects a higher nonradiative decay, probably as a result of the more distorted coordination geometry. The blue-shifting of the emission band is probably the combined result of a distortion of the coordination polyhedron and an increase of the 10Dq value. The 10Dq value is 10640 cm^{-1} for Mn(bpy) and 10720 cm^{-1} for Mn(phen); the latter is indicative of a charge-transfer state.[6c] Indeed, distortion of the phen ligand on coordination is negligible, because, as a result of its planarity, no twisting around the C2–C2′ axis is possible, in contrast to the bpy ligand.

Bathochromic shifts in the charge-transfer emission with decreasing steric constraints: The influence of the zeolite topology and cation content on the emission characteristics (Fig. 5, right) demonstrates the importance of the steric parameter in the choice of the zeolite as a cryptating agent. When the $[Mn(bpy)_2]^{2+}$ complexes synthesised in NaX zeolites (Si/Al = 1.04) are analysed with excitation at 490 nm (Fig. 5, right, spectrum a), the emission is blue-shifted to 570 nm with an increased quantum yield ($\Phi = 0.055$). When $[Mn(bpy)_2]^{2+}$ complexes are occluded within the larger EMT hypercages (Si/Al = 3.5) (spectrum c), the emission maximum is red-shifted to 591 nm with a lower quantum yield ($\Phi = 0.033$).[16a–b] The increase of the Si/Al ratio, with concomitant reduction of cation exchange capacity (CEC) and hence reduction of Na^+ ion content in the large cages, provides more free space for the encapsulated complexes. The decrease in interaction between the anion radicals and the framework cations causes red-shifting of the emission band. The metal complexes show rotational mobility when the they are hydrated;[7] this is lost upon dehydration. Consequently all faujasite-occluded complexes are blue-shifted and the decay time is reduced in the absence of the water mantle.[7–8] However, the single ligand localised anions of the MLCT state are stabilised by the charge-compensating Na^+ ions that are present; this effect decreases in the order X > Y > EMT.

The MLCT transitions are also strongly influenced by the difference in σ-donor and π-acceptor properties of the ligands. The electrons are promoted into the π^* levels of a single bpy or phen ligand and not delocalised over the two ligand orbitals, as the electron hopping process would require an energy of about 1000 cm^{-1}.[7–8] Time-resolved measurements with 355 nm radiation show decay times between 7.5 and 11.5 ms for the $[Mn(bpy)_2]^{2+}$-NaY complexes. This is longer than the 1.7 ms decay time of the quartet–sextet transition of sulfur-coordinated Mn^{2+}.[2c] For these nondehydrated occluded complexes the decay can be modelled by a single exponential. Other authors[8] have shown that rotational mobility of the complex is reduced upon dehydration, and multiexponential or Gaussian decay models should be used, since dehydration results in direct interaction of complex and surface, creating different environments for the complexes.

Discussion

The nature of the ground and excited states of metallodiimine complexes: The data presented above confirm the general concept of charge transfer related emission properties of ligand-excited species stabilised inside zeolite cages. In photophysical studies of the excited states of organic molecules or complexes of transition metal ions (TMI) the most extensively studied species are the d^3 and d^6 octahedral complexes and the d^8 square-planar complexes because of their usually inert ground state. The polypyridine complexes of Ru^{II}, Os^{II}, Cr^{III}, Rh^{III} and Ir^{III} complexes[5i] are reported to luminesce strongly in solution at room temperature and to exhibit good photosensitisation capacity for electron- and energy-transfer processes.

The position of the luminescence observed in our spectra is quite analogous to that of other Mn^{II} complexes such as

$[Mn(OMPA)_3(ClO_4)_2]$,[2c] which show a broad phosphorescence band at room temperature centred at 585 nm. The increase of the 10 Dq value for Mn(phen) compared to Mn(bpy) complexes agrees with the blue-shifting of the emission band and is indicative of CT states. The decay time of this emission is only slightly longer than the 1.7 ms quartet–sextet transition observed for S-coordinated Mn^{2+}.[2c]

The results obtained shed new light on the influence of zeolite topology and the nature of the ligand; these factors have a profound influence on the emission characteristics of zeolite-occluded TMI complexes.

Steric restrictions imposed by the FAU and the EMT topologies on the occluded complexes differ significantly: Within the FAU topology the free space in the supercages varies significantly with the number of charge-compensating cations. Moreover, when the zeolite is dehydrated at around 473 K, Na^+ ions remain partially hydrated. Thus, effects of stabilisation might result from the proximity of the positive charge and associated water.

All emission experiments reported in the literature have been performed on Ru complexes encapsulated in NaY. Although effects of cation loading and degree of hydration could be monitored, effects of topology and of density of the charge-compensating ions could not be taken into account. For water saturations of up to 80%, a nonlinear relationship between emission intensity and water content was observed.[7a] For higher degrees of hydration, emission is quenched.[7a] Destabiliation of the π^* orbital due to lack of solvation causes the emission to blue-shift and the lifetime to decrease.[8b]

The occupancy of CT states in the present samples is consistent with the observed blue shift in the emission as the ligand is varied, although the effect is too big to be assigned entirely to an increase in 10 Dq . An extra steric factor needs to be taken into account.

A blue shift is observed when the ligand favours distortion in the coordination sphere (phen), or when the zeolite topology is changed, or when the amount of hydrated cations is increased according to the sequence EMT < Y < X. This ipsochromic shift can be explained in terms of a ligand- or matrix-induced distortion of the complex. Thomas et al. showed that steric restriction causes a blue-shifting of $[Ru(bpy)_3]^{2+}$ incorporated into a polymerised silica.[14] A marked blue shift is observed with respect to that of species adsorbed at the surface. The hypercage of EMT is bigger than the supercage of FAU. In the FAU supercage, free space can be further restricted by an increasing number of (hydrated) Na or charge-compensating cations, caused by a decreasing Si/Al framework ratio. This steric effect is operative in the materials investigated here. Apart from steric effects, ion pairing between Na^+ ions and organic radical anions can have an effect on the emission and can stabilise the π^* ligand orbitals. Na^+ stabilisation of the π^* orbitals is evident from the observed red shift in pyrenes adsorbed in NaY and NaX.[17b] Thus, in the present case the steric effect or the effect of matrix-induced distortion (blue shift along the series EMT, Y, X) is dominant over the effect of ion-pair or ion-triplet formation (red shift going from Y to X zeolite).

Whereas pyrenes are flat molecules, bisdiimine complexes are almost spherical; this makes the latter more sensitive to steric influences. For the sequence EMT, Y, X, the average number of water molecules per Na^+ should decrease; less O–H vibrations will therefore be available to couple with the excited complex and assist in radiationless transition from ligand H atoms, and the quantum yield will thus increase. An analogous increase in quantum yield has been reported on substitution of D_2O for H_2O.[10c]

The mechanism of emission involves a charge-transfer state: The distinction between d–d-related emission and CT-related emission is a complex issue, as has been pointed out for $[Ru(bpy)_3]^{2+}$.[5] The emission was initially attributed to a charge-transfer fluorescence;[5a] this was later disputed, and the emission was reassigned as a "d–d" phosphorescence,[5b] a "d–d" fluorescence,[5c] charge-transfer[5d–e] and charge-transfer phosphorescence.[5f] Today, consensus has grown towards a charge-transfer phosphorescence mechanism (i.e., ^{3}MLCT → ground state).[5g] Furthermore, the MLCT state was found to be localised,[10d] and symmetry groups and CT characteristics for ground and excited states of $[Ru(bpy)_n]^{2+}$ were studied.[5h]

Mn^{II} complexes have five unpaired electrons in the d orbitals in a pseudospherical (d^5) configuration, and Mn^{II} has a high-spin $^6A_1$ ground state (Fig. 7). Excitation to a $^4T_1$ state is followed by the population of a ^{4}CT, which is converted by inter-

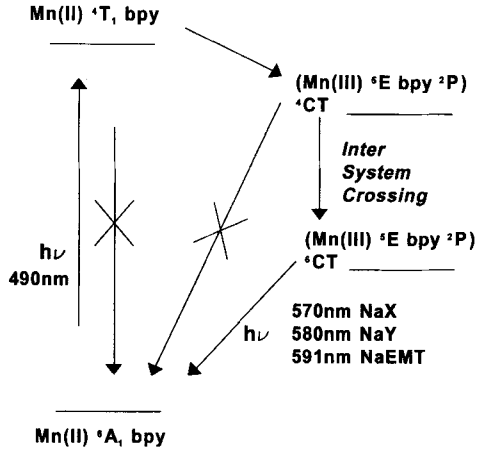

Fig. 7. Scheme of the excited states proposed for the zeolite-occluded Mn/α-diimine complexes.

system crossing to a ^{6}CT state from which emission occurs. Mixing of the ^5E state of Mn with the ^2P state of bpy results in a $^{4/6}$CT state. The ^{6}CT complex with an α-diimine radical, when formed in the zeolite, does not dissociate, in analogy with $[Ru(bpy)_3]^{2+}$-NaY.[8–9] MLCT ligand-centred radicals of complexes such as $[Mn(bpy)(CO)_3]$[4] have a π^* SOMO. For a mono-Mn(bpy) complex the radical is evidently localised at a single ligand.[4] For bis- or tris-$[Ru(bpy)_n]^{2+}$ the single ligand localised nature of the radical was probed by excited-state resonance Raman,[15a] transient absorption,[15a] EPR[15b] and flash fotolysis.[15c–e] The emission decay times of the $[Mn(bpy)_2]^{2+}$-NaY complexes are significantly longer than those of $[Ru(bpy)_2]^{2+}$-NaY (98 ns at high complex loading; 440 ns at lower complex loading).[8b] The intersystem crossing to the ^{6}CT state is followed by the emission from the ^{6}CT state to the $^6A_1$ ground state. Only a preceding ^{6}CT can be responsible for the very long decay times of the luminescence of the Mn^{II}/α-diimine radical system.

Complexes with labile states can be made luminescent when the ligand is enclosed in a suitable cage ligand: An example of this is the well-defined coordination spheres formed by bpy·bpy·bpy cryptates.[12a] Also zeolite cages impose steric constraints on ligands so that they cannot move away from the TMI. Zeolites thus function as supramolecular cryptating agents that enhance coordination sphere stability, which critically protects the complex against photodissociation. "Forced" inertness imposed on TMI complexes by intrazeolitic encapsulation is a valuable alternative to the use of organic cage-type ligands.[12]

0947-6539/96/0205-0596 $ 15.00+.25/0 Chem. Eur. J. 1996, 2, No. 5

Acknowledgement: This work was supported by the Belgian Government in the frame of a Interuniversitary Attraction Pole (IUAP II-016 and III-040) and the FKFO. PPKG and MVDA thank the Belgian National Fund for Scientific Research for research positions as Doctoral Researcher and Director of Research, respectively. XYL thanks the support of RGC, Hong Kong, and the Hong Kong University of Science and Technology.

Received: February 1, 1995
Revised version: December 1, 1995

[1] a) P. P. Knops-Gerrits, D. E. De Vos, F. Thibault-Starzyk, P. A. Jacobs, *Nature* **1994**, *369*, 543–546; b) P. P. Knops-Gerrits, F. Thibault-Starzyk, P. A. Jacobs, *Stud. Surf. Sci. Catal.* **1994**, *84B*, 1411–1417; c) C. C. Addison, M. Kilner, *J. Chem. Soc. A.* **1966**, 1249–1254; d) S. R. Cooper, M. Calvin, *J. Am. Chem. Soc.* **1977**, *99*, 6623–6630; e) S. R. Cooper, G. C. Dismukes, M. P. Klein, M. Calvin, *ibid.* **1977**, *100*, 7248–7258; f) J. E. Sarneski, H. Holden Thorp, G. W. Brudvig, R. H. Crabtree, G. K. Schulte, *ibid.* **1990**, *100*, 7255–7260.

[2] a) I. D. Buric, A. D. Aleksik, B. J. Draskovic, K. I. Nikolic, *Fizika* **1988**, *20*, 435–440. b) I. D. Buric, K. I. Nikolic, A. D. Aleksik, *Acta Phys. Pol. A.* **1986**, *A69*, 561–565; c) D. Boulanger, D. Curie, R. Parrot, *J. Luminesc.* **1991**, *48–49*, 680, d) J. C. Hempel, R. A. Palmer, M. C. L. Yang, *J. Chem. Phys.* **1976**, *64*, 4314–4320.

[3] a) A. D. Kirk, P. E. Hoggard, G. B. Porter, M. G. Rockley, M. W. Windsor, *Chem. Phys. Lett.* **1976**, *37*, 199–203; b) G. B. Porter, A. D. Kirk, D. K. Sharma, *J. Phys. Chem.* **1986**, *90*, 1781–1783.

[4] a) D. J. Stufkens, T. Van Der Graaf, G. J. Stor, A. Oskam, in *Photoprocesses in TM Complexes, Biosystems and Other Molecules, Experiment and Theory* (Ed.: E. Kochanski), Kluwer, Dordrecht **1992**, pp. 217–232.

[5] a) J. P. Paris, W. W. Brandt, *J. Am. Chem. Soc.* **1957**, *81*, 5001; b) G. B. Porter, H. L. Schläfer, *Ber. Bunsenges. Phys. Chem.* **1964**, *68*, 316; c) G. A. Crosby, W. G. Perkins, D. M. Klassen, *J. Phys. Chem.* **1965**, *43*, 1489; d) R. A. Palmer, T. S. Piper, *Inorg. Chem.* **1966**, *5*, 864; e) D. M. Klassen, G. A. Crosby, *J. Chem. Phys.* **1968**, *48*, 1853–1858; f) F. E. Lytle, D. M. Hercules, *J. Am. Chem. Soc.* **1969**, *91*, 253; g) J. N. Demas, G. A. Crosby, *ibid.* **1971**, *93*, 2841–2847; h) E. M. Kober, T. J. Meyer, *Inorg. Chem.* **1982**, *21*, 3967; i) K. Kalyanasundaram, *Photochemistry in Micro-heterogeneous Systems*, **1987**, Acadamic Press, New York; j) R. A. Krause, *Struct. Bonding* **1987**, *67*, 1–52; k) B. K. Ghosh, A. Chakravorty, *Coord. Chem. Rev.* **1989**, *95*, 239–394. l) V. Balzani, F. Scandola, *Supramolecular Photochemistry*, **1990**, Ellis Horwood, New York; m) V. Balzani, F. Barigelletti, L. De Cola, *Top. Curr. Chem.* **1990**, *158*, 31–71; n) F. Scandola, M. T. Indelli, C. Chiorboli, C. A. Bignozzi, *ibid.* **1990**, *158*, 73–149; o) T. J. Meyer, G. J. Meyer, B. W. Pfennig, J. R. Schoonover, C. J. Timpson, J. F. Wall, C. Kobush, X. Chen, B. M. Peek, C. G. Wall, W. Ou, B. W. Erickson, C. A. Bignozzi, *Inorg. Chem.* **1994**, *33*, 3952–3964.

[6] a) W. R. McWhinney, J. D. Miller, *Adv. Inorg. Chem. Radiochem.* **1967**, *12*, 135–215; b) E. D. McKenzie, *Coord. Chem. Rev.* **1971**, *6*, 187–216; c) A. B. P. Lever, *Inorg. Electr. Spectr.* (2nd ed.) **1984**, Elsevier, Amsterdam, p. 296; d) K. Nakamoto, *Infrared and Raman Spectra of Inorganic and Coordination compounds* (4th ed.), **1986**, 206–213, Wiley, New York; e) B. Durham, S. R. Wilson, D. J. Hogson, T. J. Meyer, *J. Am. Chem. Soc.* **1980**, *102*, 600–607; f) Z. Li, C. H. Wang, L. Persaud, T. E. Mallouk, *J. Phys. Chem.* **1988**, *92*, 2592; g) J. S. Kruger, J. A. Mayer, T. E. Mallouk, *J. Am. Chem. Soc.* **1988**, *110*, 8232; h) Y. Kim, T. E. Mallouk, *J. Phys. Chem.* **1992**, *96*, 2879.

[7] a) W. DeWilde, G. Peeters, J. H. Lunsford, *J. Phys. Chem.* **1980**, *84*, 2306–2310. b) W. H. Quayle, J. H. Lunsford, *Inorg. Chem.* **1982**, *21*, 97–101. c) W. H. Quayle, G. Peeters, G. L. De Roy, E. F. Vansant, J. H. Lunsford, *Inorg. Chem.* **1982**, *21*, 2226–2231.

[8] a) P. K. Dutta, J. A. Incavo, *J. Phys. Chem.* **1987**, *91*, 4443–4446; b) J. A. Incavo, P. K. Dutta, *ibid.* **1990**, *94*, 3075–3081; c) W. Turbeville, D. S. Robins, P. K. Dutta, *ibid.* **1992**, *96*, 5024–5029; d) M. Borja, P. K. Dutta, *Nature* **1993**, *362*, 43–46; e) P. K. Dutta, R. E. Zaykoski, *Zeolites*, **1988**, *8*, 179; f) M. Ledney, P. K. Dutta, *J. Am. Chem. Soc.* **1995**, *117*, 7687–7695.

[9] a) K. Maruszewski, D. P. Strommen, K. Handrich, J. R. Kincaid, *Inorg. Chem.* **1991**, *30*, 4579–4582; b) K. Maruszewski, D. P. Strommen, J. R. Kincaid, *J. Am. Chem. Soc.* **1993**, *115*, 8345–8350; c) K. Maruszewski, J. R. Kincaid, *Inorg. Chem.* **1995**, *34*, 2002–2006.

[10] a) G. A. Crosby, *Acc. Chem. Res.* **1975**, *8*, 231; b) F. E. Lytle, D. M. Hercules, *J. Am. Chem. Soc.* **1969**, *91*, 253; c) J. Van Houten, R. J. Watts, *ibid.* **1976**, *98*, 4853–4858; d) R. F. Dalllinger, W. H. Woodruff, *ibid.* **1979**, *101*, 4391–4393; e) P. G. Bradley, N. Kress, B. A. Hornberger, R. F. Dalllinger, W. H. Woodruff, *ibid.* **1981**, *103*, 7441–7446.

[11] a) D. E. De Vos, F. Thibault-Starzyk, P. P. Knops-Gerrits, R. F. Parton, P. A. Jacobs, *Macromol. Symp.* **1994**, *80*, 157–184; b) D. E. De Vos, P. P. Knops-Gerrits, R. F. Parton, B. M. Weckhuysen, P. A. Jacobs, R. A. Schoonheydt, *J. Inclusion Phenom.* in press; c) D. E. De Vos, E. Feijen, R. A. Schoonheydt, P. A. Jacobs, *J. Am. Chem. Soc.* **1994**, *116*, 4746–4752.

[12] J. C. Rodriguez-Ubis, B. Alpha, D. Plancherel, J. M. Lehn, *Helv. Chem. Acta.* **1984**, *67*, 2264.

[13] a) N. L. Allinger, *J. Am. Chem. Soc.* **1977**, *99*, 8127; b) D. W. Breck, *Zeolite Molecular Sieves*, John Wiley, New York **1974**, p. 85; C. M. V. Veidis, B. Dockum, F. F. Charron, Jr., W. M. Reiff, T. F. Brennan, *Inorg. Chem. Acta.* **1981**, *53*, L197–L199.

[14] a) J. Wheeler, J. K. Thomas, *J. Phys. Chem.* **1982**, *96*, 4540; b) W. J. Albery, P. N. Barlett, C. P. Wilde, J. R. Darwent, *J. Am. Chem. Soc.* **1985**, *107*, 1854.

[15] a) R. F. Dalllinger, W. H. Woodruff, *J. Am. Chem. Soc.* **1979**, *101*, 4391–4393; b) A. G. Motten, K. Hanck, M. K. DeArmond, *Chem. Phys. Lett.* **1981**, *79*, 541; c) U. Lachish, P. P. Infelta, M. Grätzel, *Chem. Phys. Lett.* **1979**, *62*, 317; d) R. V. Benason, C. Salet, V. Balzani, *R. Acad. Sci. Ser. B.* **1979**, *289*, 41; e) C. Creutz, M. Chou, T. L. Netzel, M. Okumura, N. Sutin, *J. Am. Chem. Soc.* **1980**, *102*, 1309.

[16] a) E. J. Feijen, K. De Vadder, M. H. Bosschaerts, J. L. Lievens, J. A. Martens, P. J. Grobet, P. A. Jacobs, *J. Am. Chem. Soc.* **1994**, *116*, 2950–2957; b) Whereas the FAU supercage is composed of four 12 MR windows, there are five 12 MR windows in the EMT hypercage; as a result the hypercage is larger, and less interaction of charge-compensating lattice cations with the complexes occurs; c) F. Delprato, L. Delmotte, L. J. Guth, L. Huve, *Zeolites* **1990**, *10*, 546–552; d) J. L. Lievens, J. P. Verduijn, A. J. Bons, W. J. Mortier, *ibid.* **1992**, *12*, 698–705.

[17] a) K. B. Yoon, *Chem. Rev.* **1993**, *93*, 321; b) V. Ramamurthy, J. V. Kaspar, *Mol. Cryst. Liq. Cryst.* **1992**, *211*, 211–226.

[18] a) V. K. Kaushik, S. G. T. Bhat, D. R. Corbin, *Zeolites*, **1993**, *13*, 671; b) N. Herron, *J. Coord. Chem.* **1988**, *19*, 25–38.